Molecular Crystals
Publication details, including instructions for authors and subscription information:
http://www.tandfonline.com/loi/gmcl15

Photo-Enhanced Electron Emmision from Alkali Metal Contacts into Anthracene

A. Many [a] , J. Levinson [a] & I. Teucher [a]
[a] The Hebrew University, Jerusalem, Israel
Version of record first published: 21 Mar 2007.

To cite this article: A. Many , J. Levinson & I. Teucher (1969): Photo-Enhanced Electron Emmision from Alkali Metal Contacts into Anthracene, Molecular Crystals, 5:3, 273-294

To link to this article: http://dx.doi.org/10.1080/15421406908083461

Molecular Crystals. 1969. Vol. 5, pp. 273–294

Printed in Great Britain

Photo-Enhanced Electron Emmission from Alkali Metal Contacts into Anthracene†

A. MANY, J. LEVINSON and I. TEUCHER

The Hebrew University,
Jerusalem, Israel

Received October 21, 1968; *in revised form November* 20, 1968

Abstract—Dark- and photo-current measurements are used to study trap characteristics and optical de-trapping processes in anthracene samples provided with alkali and alkaline-earth metal contacts. The spectral response of the photocurrent yield in the entire photon-energy range studied (0.95–3.4 eV) originates from optical excitation of electrons from a single discrete set of traps which is continuously filled by electron injection from the active metal contact. The traps are 0.95 eV deep and are present with a density of about 10^{13} cm^{-3}. De-trapping appears to occur by direct photoexcitation into the conduction band at long wavelengths and by interaction of occupied traps with triplet and singlet excitons at shorter wavelengths. The spectral yield curve exhibits considerable structure which can be advantageously used to study the various electronic-vibronic states in anthracene.

Introduction

The investigations reported here are mainly concerned with studies of the dark and photo-enhanced currents in anthracene samples provided with alkali or alkaline-earth metal contacts. Such contacts can inject electrons into anthracene[1,2] which are mostly trapped, and photocurrent measurements provide important information on the trap characteristics and on the optical transitions involved in the de-trapping process. The spectral response of the photocurrent yield varies over seven orders of magnitude in the photon energy range 0.95–3.4 eV. Starting

† The research reported herein has been sponsored in part by the European Research Office, U.S. Army, Frankfurt-am-Main, Germany.

from a threshold of 0.95 eV, the yield exhibits a slightly undulating linear rise up to a photon energy of about 1.75 eV. This is followed by a series of four well defined peaks in the range 1.8–2.7 eV leading, after a very steep rise, to a multi-structured peak centered at about 3.1 eV.

It has been established that the *entire* spectral yield curve observed originates from optical excitation out of a single discrete set of traps situated 0.95 eV below the conduction-band edge and present with a density of about 10^{13} cm^{-3}. *Direct* optical excitation from this trapping level into the conduction band appears to be responsible for the initial, nearly linear response of the photocurrent yield. The small structure apparent in this range suggests that excitation takes place into a system of narrow bands, about 0.2 eV apart, resulting probably from the interaction of molecular vibrations with a narrow electronic band. The four peaks in the range 1.8–2.7 eV and the one at $\sim$3.1 eV very likely arise from de-trapping[3,4] by triplet and singlet excitons, respectively. The fine structure exhibited by the latter peak must be due to electronic-vibronic levels of the singlet state involving many vibrational modes.

Experimental

The single-crystal anthracene platelets used were grown by the following procedure. The starting material is first dissolved in ethylen glycol and the solution is distilled twice. After precipitation, the anthracene powder is zone refined 30–40 times in an atmosphere of argon (4–10 cm pressure). The purified material is then placed at one end of a closed tube in an atmosphere of 12 cm argon. The tube is moved at a rate of about 2 mm per hour through a furnace having a very strong temperature gradient (peak temperature 150–200 °C). At the end of the growth process (about 24 hours), many crystal platelets are sublimated at the other end of the tube. Out of these, several platelets of high perfection having typical dimensions of 10 × 10 mm^2 in area and 20–100 microns in thickness can be selected.

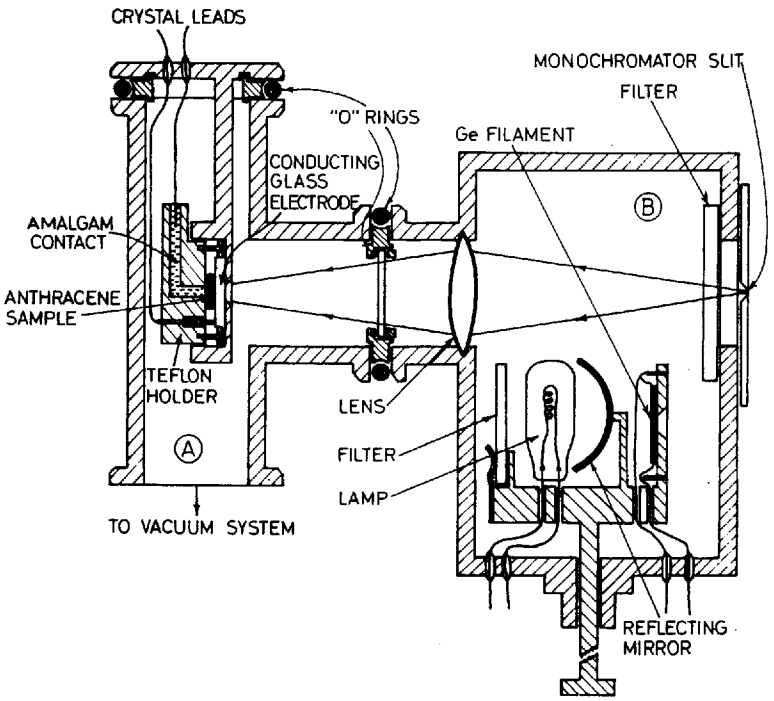

Figure 1. Vacuum chamber and part of optical system used for photocurrent measurements.

Fig. 1 is a schematic diagram of the vacuum chamber used in the measurements. The anthracene platelet is enclosed in a sandwich-type cell which consists, on the one side, of a teflon block having an L-shaped cavity of circular cross section, and of a conducting glass electrode on the other. Illumination of the sample is effected through the glass electrode which is almost completely transparent in the spectral range studied ($\lambda > 0.38\,\mu$). The anthracene sample is tightly pressed against the cavity. Any deformation caused by such pressing is confined mostly to the periphery of the crystal plate. Thus, the central region of the crystal, which is the only region of interest, remains essentially undamaged. At this stage an amalgam of the alkali or alkaline-earth metal or a 50% Na–K liquid alloy is introduced through the

upper end of the L-shaped cavity, filling most of it. The cell is then shaken lightly so as to ensure that an unoxidized layer of the active metal is in contact with the crystal surface. The large quantity of amalgam present acts as a protecting medium against oxidation of the interface layer. It was found that when the cell is kept under vacuum of $10\,\mu$, the injecting properties of the contact do not deteriorate even a few weeks following the assembly of the cell.

The area of the metal contact in the sandwich-type cell is 0.1 cm^2. All current values reported below correspond therefore to current *densities* that are numerically ten times larger.

The cell is mounted inside the vacuum chamber which is simply a Leybold T-shaped junction (A in Fig. 1). The lower end of the junction is connected into a vacuum system. The cell holder is attached to a metal plate at the upper end of the chamber, which contains also the vacuum-tight lead seals. The right-hand side of the chamber is sealed by a quartz window. This end is adjacent to another chamber (B) which, in turn, is attached to the monochromator slit. A lens is used to image the slit onto the anthracene sample. There are provisions (not shown) to interpose between the slit and the lens selective filters in order to eliminate stray light, as well as grey filters to vary the light intensity. Chamber B includes an air-cooled reflector lamp with a suitable filter which can be moved up to face the lens for direct (polychromatic) illumination of the sample. In this position the light from the monochromator impinges on a germanium filament which is used to measure the spectral light intensity.

The optical system consists of a 150 W Tru-flector Sylvania lamp and a Hilger D246 monochromator. The dc voltages applied across the sample are derived from a battery bank. The dark currents and photocurrents are measured by a Cary Model 31 electrometer and are recorded by a Sunvic recorder.

Results

With a dc voltage applied, of a polarity such as to make the metal negative, appreciable photocurrents are observed in the

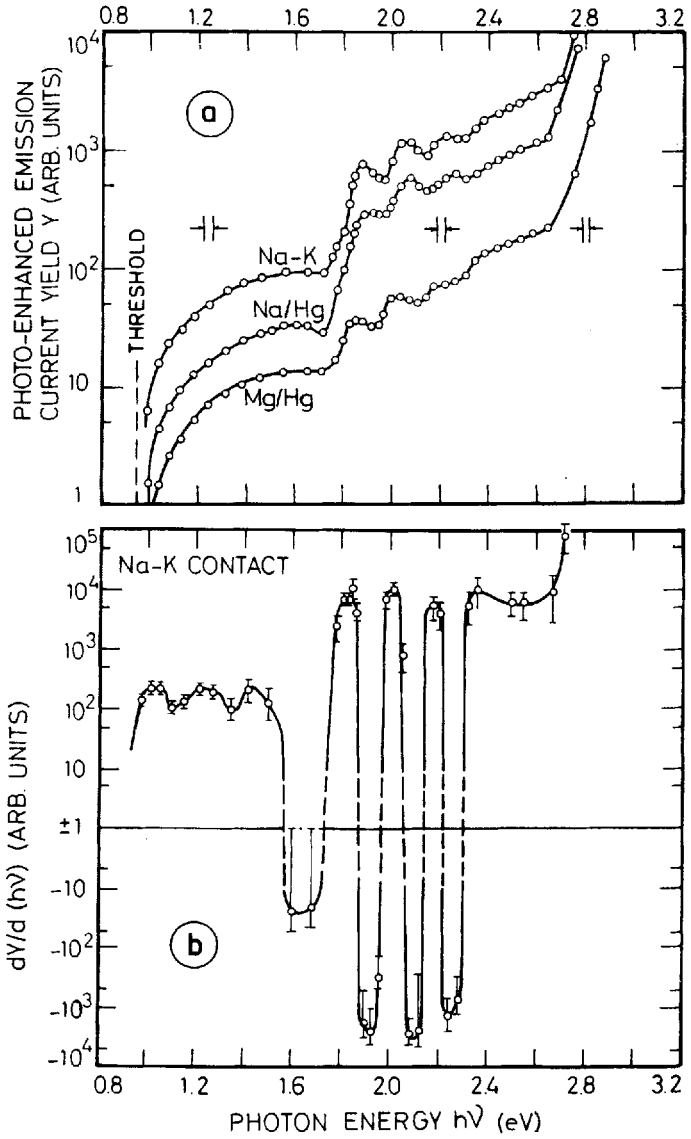

Figure 2. (a) Photo-enhanced emission-current yield Y *vs.* photon energy $h\nu$ for Na–K alloy and for Na and Mg mercury-amalgam contacts on anthracene. (b) $dY/d(h\nu)$ *vs.* $h\nu$ for the Na–K contact. Margin of error marked off for each point.

range 1.3–0.38 μ. That these originate from the active metal is established by the fact that the photocurrents for a pure mercury electrode are at least one to two orders of magnitude lower. Typical results of the spectral response of the photocurrent yield Y (current per incident photon) are shown in Fig. 2(a) for three metal contacts. Similar curves were obtained with mercury amalgams of Li and Ca. A striking feature of the data is the similarity in shape of all curves: the energy positions of the photocurrent threshold and of the various peaks are the same to within $\pm$ 0.03 eV, being independent of the alkali or alkaline-earth metal used. The reason for this is that all the contacts used are injecting and, as will be shown below, the photocurrent response is solely determined by the anthracene trap characteristics. The logarithmic scale used in displaying the large variation in the yield is too condensed to reveal all the features present in the curves. The structure is better seen by plotting the derivative of the yield with respect to photon energy, as shown in Fig. 2(b) for the case of the Na–K alloy contact. Starting from a threshold of 0.95 eV (see also Fig. 3 below), the derivative reveals first a broad undulating plateau. This is followed by four pronounced peaks which are clearly seen also in the yield curve itself (Fig. 2(a)). The rapidly rising portion of the curve leads to a multi-structured peak centered around 3.1 eV (see below).

The logarithmic scale used in Fig. 2(a) is inadequate also to describe conditions near the threshold energy. Plots of the spectral response of Y in this range are shown in Fig. 3 on a linear scale for the same three metal contacts. The experimental points are seen to lie on nearly straight lines which extrapolate to a common threshold of 0.95 eV. This threshold is independent of the applied voltage over the entire voltage range studied (typically 50–300 V) and does not vary from sample to sample.

The results described above were at first[5] interpreted as due to direct photoemission from the alkali or alkaline-earth metal contact into the conduction band of anthracene. Similar results by Baessler *et al.*[6] and by Dressner[7] were interpreted on the same basis. However, the data presented below show conclusively that in our

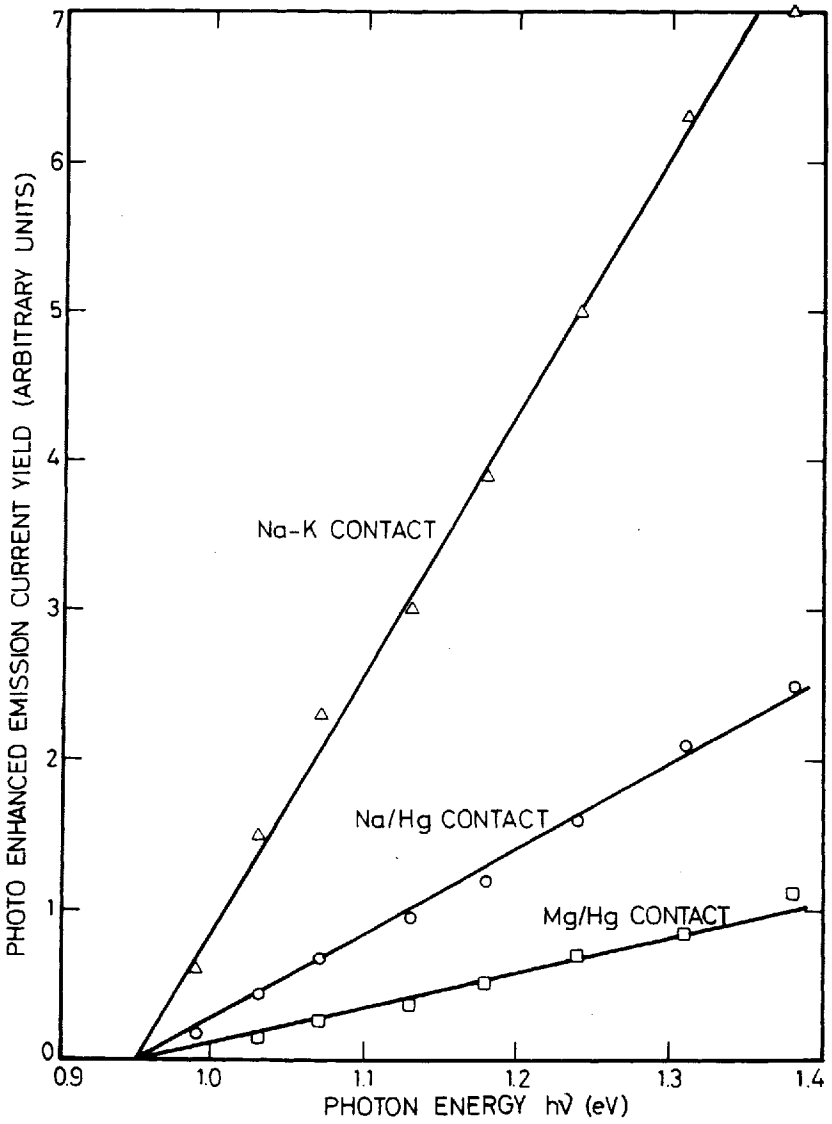

Figure 3. Photo-enhanced emission-current yield Y *vs.* photon energy near threshold.

case at least photo-excitation out of bulk traps, which are continually being filled by injected electrons, rather than direct photoemission from the active metal is the dominant underlying process. As pointed out by Mehl[8] in connection with the work of Baessler *et al.*[6] we believe that bulk traps play the major role in the results of these authors as well as in those of Dressner,[8] but this question will be discussed elsewhere. Here we shall be mostly concerned with the characteristics of the traps and with the mechanism of de-trapping by light.

It was observed that *after* a spectral yield curve of the type shown in Fig. 2(a) had been taken, the photocurrent measured in the reverse direction (active metal *positive*) exhibited a spectral response of almost identical form. Furthermore, just the application of a " forward " voltage is sufficient to give rise to such a " reverse " photocurrent. (The terms " forward " and " reverse " will be used throughout as corresponding to the active metal being negative and positive, respectively.) It is thus immediately obvious that the reverse photocurrent must be due to photo-excitation of electrons from traps which have been filled up by injection from the active metal during the prior application of the forward voltage.

Emission of electrons from the traps into the conduction band by *thermal* processes is extremely slow, as indicated by the observation that if the sample is kept in the dark the magnitude of the reverse photocurrent decreases by less than 10% over a period of 15 hours. As expected, however, the reverse current decays with time of illumination. Such bleaching is a result of the gradual de-trapping of electrons by the light, and by the time all the previously injected electrons have been photo-excited into the conduction band and swept out, the sample returns to its virgin, non-photoconductive state. Bleaching experiments are depicted in Fig. 4. The top curve represents the spectral yield of the photo-enhanced emission from a Na/Hg contact in the *forward* direction, and is very similar to the corresponding curve in Fig. 2(a). The curve below (" unbleached ") is the spectral yield obtained from the *reverse* current following injection (in the forward direction)

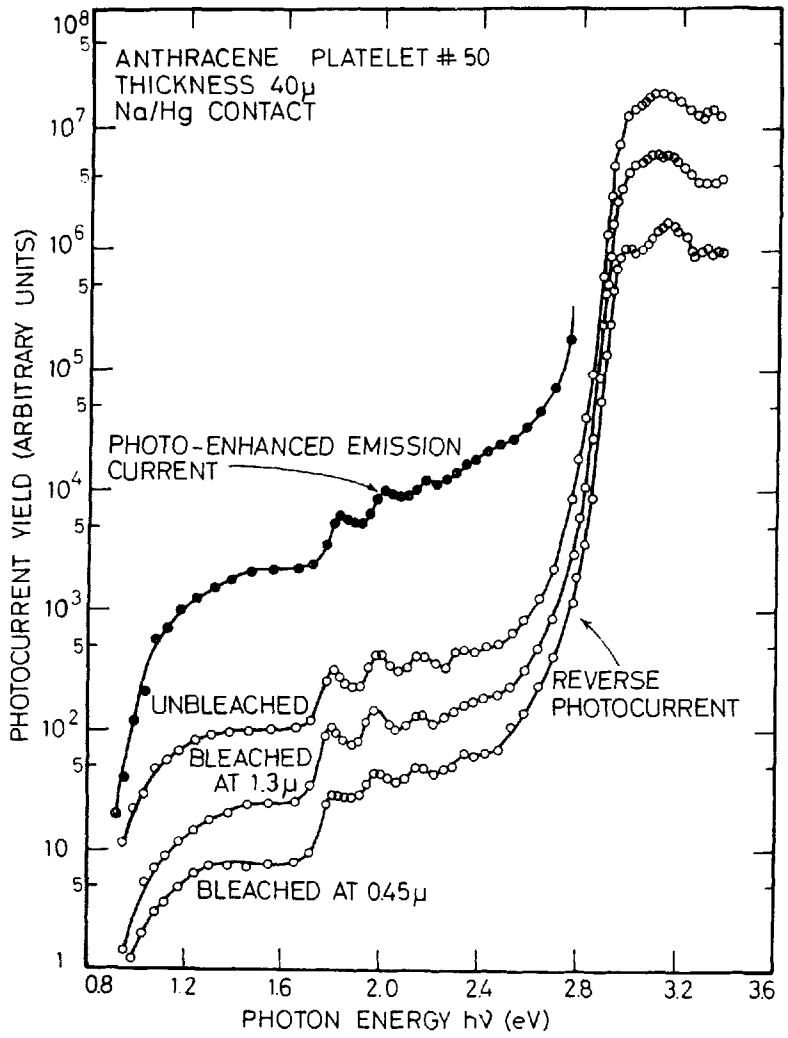

Figure 4. Spectral response of photocurrent yield in forward direction (upper curve) and in reverse direction (lower three curves).

at 180 V. Very low light intensities had to be used in taking such curves because of bleaching. The measurements could be extended in this case all the way to the absorption region since the

occurrence of bleaching makes it easy to differentiate unambiguously between the photocurrent due to de-trapping and the photocurrent that may arise in this region from intrinsic bulk processes. (Actually, under the conditions of the experiment, the former photocurrent is at least ten times larger.) It is seen that the spectral response of the reverse photocurrent yield reproduces quite closely, both in form and in structure, that of the forward photocurrent. That essentially only one discrete set of traps is involved in the de-trapping process follows from the observation that bleaching by light of 1.3 μ ($h\nu \approx 1$ eV), or in fact by monochromatic light of any other wavelength in the range of 1.3–0.38 μ, lowers the *entire* spectral yield curve by practically the *same* factor. This is shown by the two lower yield curves of Fig. 4, which represent the spectral response of the reverse current following partial bleaching at two extreme wavelength values. (As was pointed out earlier, the measurements were carried out under sufficiently low light intensities, so that negligible bleaching occurred *during* the measurement of each curve.) The fact that bleaching by photons of energy 1 eV is able to uniformly reduce the reverse photocurrent at *higher* photon energies immediately indicates that deeper traps do not contribute to the process. Traps shallower than 0.95 eV are ruled out by the absence of any photocurrent at wavelengths longer than ~ 1.3 μ.

The reverse photocurrent in the photon-energy range of 2.9–3.4 eV displays considerable structure which is not revealed on the condensed scale of Fig. 4. In Fig. 5 the unbleached and partially-bleached spectral-response curves obtained (from a different experiment) for this range is shown on a much more expanded scale. The measurement of the unbleached curve was taken with a monochromator slit width of 0.02 mm so that the spectral resolution is better than several Ångstroms. The fine structure revealed, although small in amplitude, is definitely real.

More detailed results of the bleaching efficiency under illumination at different wavelengths have been obtained by the following experiment. The traps were first filled by injection in the forward direction at 180 V for a fixed period of time. Next, the sample is

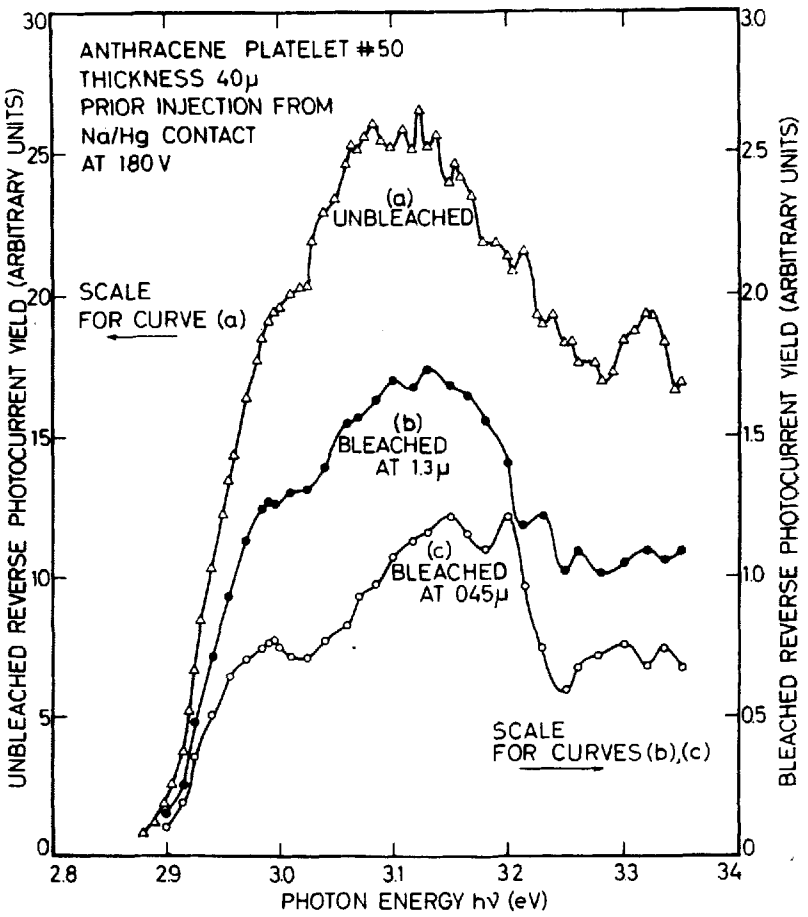

Figure 5. Spectral response of reverse photocurrent in the singlet absorption region.

illuminated by a *fixed* dose of incident photons at a given wavelength. The bleaching efficiency at this wavelength is then obtained by measuring the relative reduction in the reverse photocurrent (at $1\,\mu$) with respect to the initial, unbleached value. In Fig. 6, the bleaching efficiency (as measured at $1\,\mu$) is plotted against the photon energy of the bleaching light. As to be expected for the case of a discrete trapping level, the curve again reproduces the shape and structure

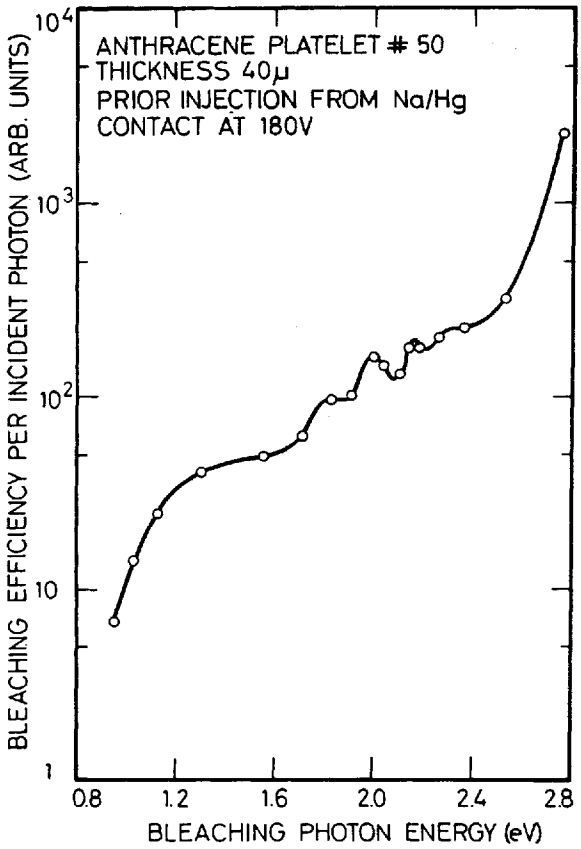

Figure 6. Bleaching efficiency (as measured at 1 μ) against photon energy of bleaching light at constant dose of photon flux.

of the spectral yield of the photo-enhanced emission current and of the reverse photocurrent Figs. 2 and 4).

The voltage dependence of the reverse photocurrent at two wavelengths is shown in Fig. 7. The photocurrent at zero applied voltage arises from the polarization field set up by the prior injection. Both curves are seen to start out linearly and to saturate at higher voltages ($\gtrsim$ 150 V). The field E_c at which the transition from linear to saturation conditions occurs is about 4×10^4 V/cm. This means that at this field the electron Schubweg

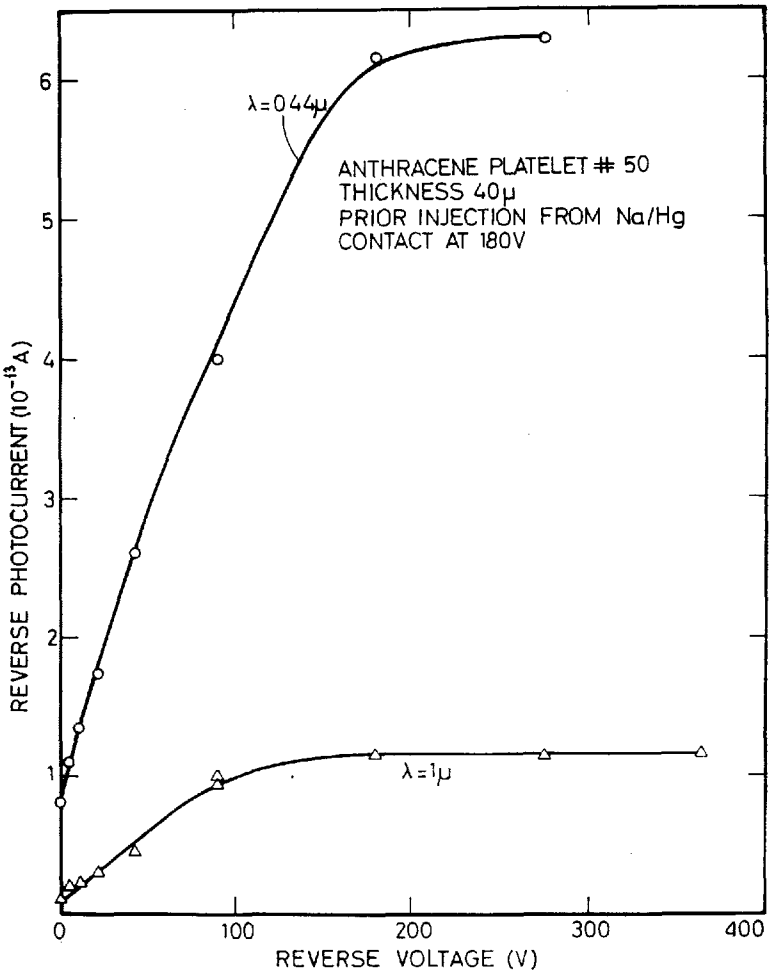

Figure 7. Voltage dependence of reverse photocurrent at two wavelengths.

$\mu_n E_c \tau$, where μ_n is the electron mobility and τ the trapping time, is comparable to the sample's length L. Using the value[9] of 0.4 $cm^2/V \cdot sec$ for μ_n, one obtains an estimate of 0.2 μsec for the trapping time.

The light-intensity dependence of the saturated reverse photocurrent measured at two wavelengths is shown in Fig. 8. The

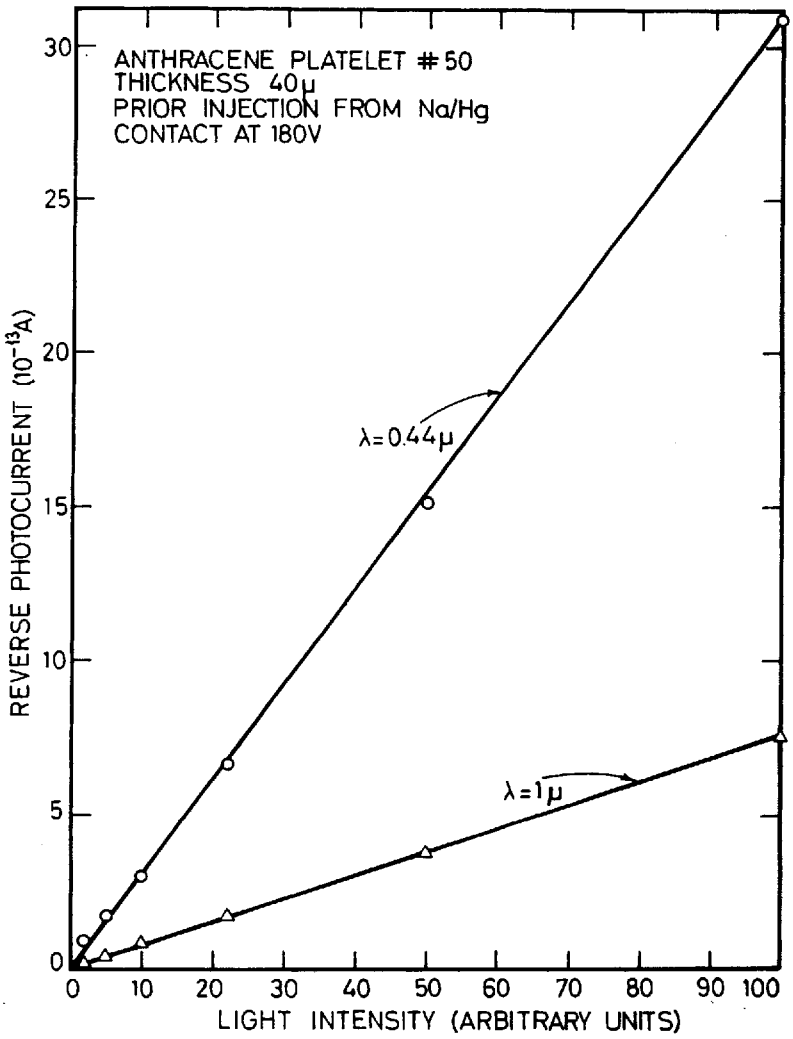

Figure 8. Light-intensity dependence of saturated reverse photocurrent at two wavelengths.

direct proportionality between photocurrent and light intensity indicates that no non-linear photo-generation effects are involved in the de-trapping process (see below).

A fairly accurate determination of the density of traps responsible for the reverse photocurrent is provided by the data in Fig. 9. Here the time decay of the saturated reverse photocurrent is followed *during* the bleaching process and is plotted on a semi-log scale for bleaching at $\lambda = 1\,\mu$ and at$\lambda = 0.46\,\mu$. The light intensities for the two wavelengths have been adjusted so as to give comparable photocurrents. The experimental points are seen to lie on straight, nearly parallel lines, indicating that the decay is exponential and that the decay constant is essentially the same for both wavelengths.

This behavior can be accounted for as follows. On the assumption that there is only one type of traps, the rate of electron de-trapping can be expressed as $dN/dt = -CFN$, where C is a proportionality constant, F is the incident photon flux and N is the number of occupied traps in the sample at time t. The linear dependence of dN/dt on F follows from the observed proportionality between the reverse photocurrent and the light intensity (Fig. 8). One thus obtains that $N = N_0 \exp(-CFt)$, where N_0 is the initial number of occupied traps in the sample. The results in Fig. 9 were obtained following prior injection at 180 V. At this voltage, the electron Schubweg is larger than the sample length (see Fig. 7 above), so that the trapped electrons are nearly uniformly distributed within the sample. Moreover, the reverse current is measured under saturation conditions, so that essentially all electrons that are de-trapped are entirely swept out of the sample. Under these two conditions the saturated photocurrent is given by $I = -\frac{1}{2}q(dN/dt)$, where q is the electronic charge. Hence $I = I_0 \exp(-CFt)$, where $I_0 = \frac{1}{2}qN_0CF$, which accounts for the observed exponential decay. Furthermore, the fact that both the initial values and the slopes of the two straight lines in Fig. 9 are, respectively, nearly the same, indicates strongly that N_0 is equal in the two bleaching experiments. (Obviously, if more than one type of traps were involved, one would not have expected an exponential decay to begin with.) The use of the relation $N_0 = 2I_0/qCF$, with CF determined from the slopes of the straight lines and I_0 given by the initial value of the current, yields

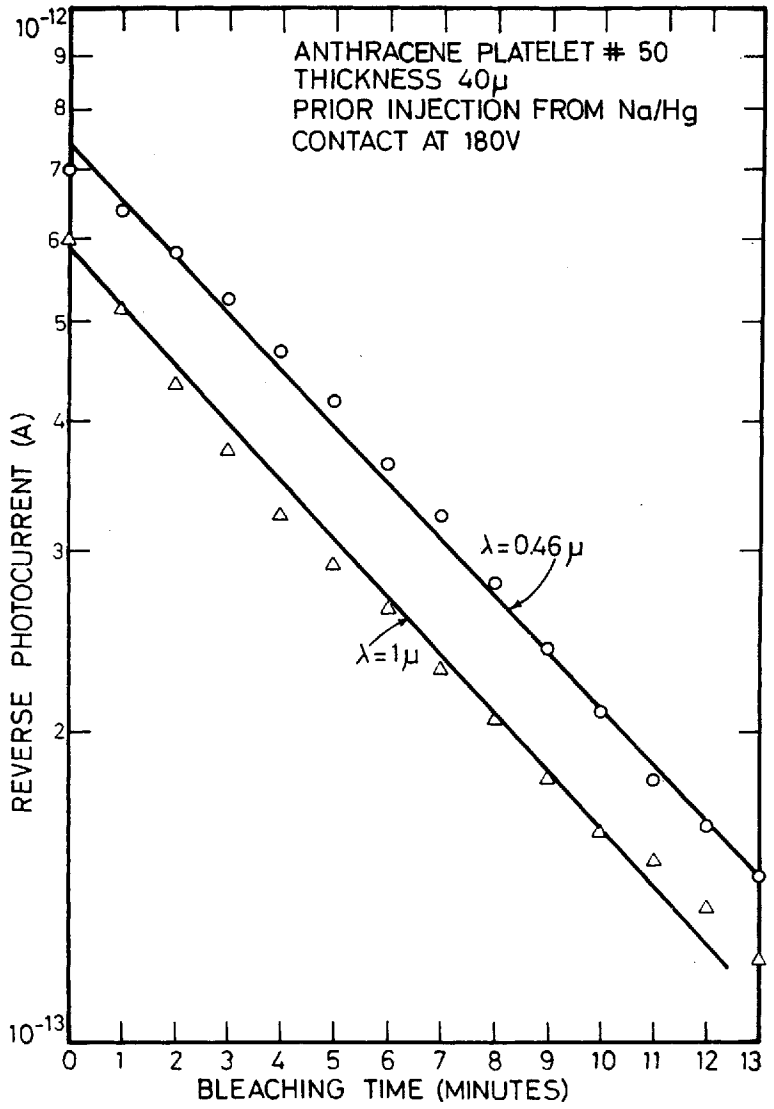

Figure 9. Semi-log plot of reverse-photocurrent decay under bleaching at two wavelengths.

$N_0 = 4.5 \times 10^9$. Dividing this value by the volume of the sample ($0.1 \times 40 \times 10^{-4}$ cm^3) one obtains for the trap density $N_t \approx 10^{13}$ cm^{-3}.

An independent determination of the trap density is provided by current–voltage measurements. The middle curve in Fig. 10 describes the voltage dependence of the *dark* current injected from a Na/Hg contact. The superlinear relation is typical to space-charge-limited currents[10] and is similar to the curves obtained by other workers[1,2,8] with alkali-metal contacts. At low voltages the current is controlled by traps, the effective value of the ratio θ of free to trapped electron density[10] being very small compared to unity. Starting at about 80 V, however, the current rises much more steeply. The steep rise signifies the rapid filling up of a set of deep traps which, as will be shown in a moment, is the one responsible for the forward and reverse photocurrents. The trap-filled limit[10] V_{TFL} (≈ 80 V) associated with these traps provides a good estimate for their density N_t. To within a factor of two or so, N_t is given[10] by $(2\epsilon_0\kappa/qL^2)V_{\mathrm{TFL}}$, where ϵ_0 is the permitivity of free space, κ is the relative dielectric constant and L the sample's thickness. Using the values $\kappa = 4$, $L = 40\ \mu$ and $V_{\mathrm{TFL}} \approx 80$ V, one obtains $N_t \approx 2 \times 10^{13}$ cm^{-3}, which is in good agreement with the value derived above from the decay characteristics of the reverse photocurrent.

The upper curve in Fig. 10 represents the voltage dependence of the current measured under (weak) illumination at $0.68\,\mu$. Illumination enhances the current by reducing the charge localized in traps as discussed above. The total space charge present in the sample under a given voltage is not changed by illumination, being essentially determined by the applied voltage only, but the ratio θ of free to trapped electron density is increased, leading to a higher current. Thus, the photocurrent in the forward direction is in effect a photo-enhanced emission current from the active metal contact and has so been termed in the discussions above. It should be noted that the photo-enhancement at voltages exceeding the trap-filled limit V_{TFL} is negligible. This is just as expected since for $V > V_{\mathrm{TFL}}$ the space-charge-limited current is

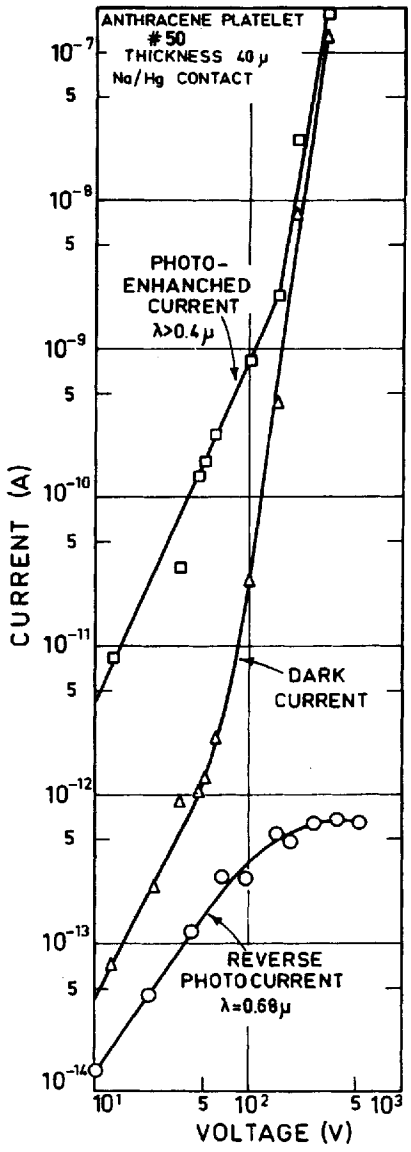

Figure 10. Log-log plots of dark and photo-enhanced emission current and of reverse photocurrent as functions of injecting voltage.

no longer controlled by the set of deep traps giving rise to the photocurrent.

More direct evidence that the deep traps discussed above are responsible for the reverse photocurrent is provided by the bottom curve of Fig. 10. This curve represents the reverse photocurrent at a *fixed* reverse voltage (180 V) as a function of the forward voltage used for prior injection from the Na/Hg electrode. The marked saturation reached at high injecting voltages by the reverse current, and hence by the number of trapped electrons, is a clear indication that all available traps contributing to the photocurrent had been completely filled up. Moreover, the transition point between the linear and saturation regimes (~ 80 V) matches quite well the trap-filled limit determined from the dark-current curve.

Discussion

The data presented above show that in the anthracene samples used the photo-enhanced emission currents from alkali or alkaline-earth metal contacts as well as the reverse photocurrents originate from photoexcitation out of a single discrete set of traps. These traps are situated 0.95 eV below the lowest conducting state of anthracene and present with a density of approximately 10^{13} cm^{-3}. There has been some evidence,[11] derived from space-charge-limited current measurements, pointing to the existence of an exponential rather than discrete electron trap distribution in anthracene. In fact the data in Fig. 10 can be analyzed on this basis as well. We believe, however, that the other data presented are much more reliable in determining the trap distribution. The results of Figs. 3, 4 and 9 indicate that (a) the threshold photon energy is independent of applied voltage, (b) bleaching at *any* wavelength lowers the entire spectral-yield curve by practically the *same* factor and, what is perhaps most indicative, (c) the decay of the reverse photocurrent with bleaching time is *exponential* and yields the *same* density of occupied traps for all bleaching wavelengths. These combined observations show conclusively that in the samples studied the trap distribution is essentially

discrete. The origin of the traps is not known. Our findings do not rule out the presence of shallower traps having sufficiently short thermal release times so as not to affect appreciably the forward and reverse photocurrents.

The important question to answer is by what mechanism are the trapped electrons excited into the conduction band. One can envisage[4,11] two possible mechanisms in anthracene: (a) direct photoexcitation into the conduction band and (b) de-trapping by interaction with triplet or singlet excitons. In principle, the entire spectral response of the photocurrent yield (Figs. 2, 4 and 5) can result from direct photoexcitation from the discrete set of traps into various sub-bands of the conduction band (mechanism (a)). However, one notes that the positions of the four peaks in the range 1.8–2.4 eV very nearly coincide with those of the main absorption peaks of the vibrational spectrum of the first excited triplet state,[12,13] while the main peak around 3.1–3.2 eV (Figs. 4 and 5) matches well the prominent singlet absorption peak[14] (3.15 eV). This strongly indicates that de-trapping by mechanism (b) is dominant in the range 1.8–3.4 eV. The wealth of detail in the structure of the yield curve at the higher energy range depicts the interaction of the singlet state with diverse modes of molecular vibrations. Analysis of such curves should yield more detailed information on these electronic-vibronic levels than has been possible by absorption measurements.[15]

Obviously, the photocurrent at photon energies less than 1.8 eV cannot arise from either singlet or triplet excitons. Mechanism (a) is the most likely one in this range. The undulations in the plateau of Fig. 1 (b) should then reflect the structure of the lower portion of the conduction band of anthracene. Measurements of intrinsic photoconductivity[16,17] and of external photoemission[18] have established the presence of a broad, free-electron conducting state in anthracene, starting at 4.0 eV above the valence band. Theoretical calculations and the small measured electron mobility indicate that electron transport occurs in a narrow (0.01–0.1 eV), tight-binding conductivity band.[19,20] Its precise position is not known—it must be lower than 4.0 eV and is probably[18] above

3.45 eV Quite likely the broad continuum of states (0.95–1.6 eV) into which the trapped electrons are photo-excited by direct transitions comprises both the tight-binding and the free-electron bands. With the presently available resolution, the differentiation between the two cannot be reliably inferred from the data. One notes, however, that the energy separation between adjacent peaks in the plateau of Fig 2(b) is approximately 0.2 eV, which is just the value to be expected from the interaction of the principal mode of the molecular vibrations[20] with a narrow electronic band.

Acknowledgements

The authors are indebted to I. Natanson for growing the anthracene single crystals and to A. Halperin and R. C. Jarnagin for helpful discussions. Thanks are also due to the personnel of the Fine Mechanics Workshop under the direction of A. Shirizly for constructing the vacuum chamber, and to I. Aharonov and Y. Arieh for their technical assistance.

REFERENCES

1. Helfrich, W., and Schneider, W. G., *Phys. Rev. Letters* **14**, 229 (1965).
2. Mehl, W., and Funk, B., *Phys. Letters* **25A**, 364 (1967).
3. Jansen, P., Helfrich, W., and Riehl, N., *Phys. Stat. Sol.* **7**, 851 (1964).
4. Adolph, J., *Helv. Phys. Acta* **38**, 409 (1965).
5. Many, A., Levinson, J., and Teucher, I., *Phys. Rev. Letters* **20**, 1161 (1968).
6. Baessler, H., and Vaubel, G., *Solid State Comm.* **6**, 97 (1968). Baessler, H., Riehl, N., and Vaubel, G., *Phys. Stat. Sol.* **26**, 607 (1968).
7. Dresner, J., *Phys. Rev. Letters* **21**, 356 (1968).
8. Mehl, W., *Solid State Comm.* **6**, 549 (1968).
9. Kepler, R. G., in *Phonons and Phonon Interactions*, T. A. Bak, Editor (Benjamin, N.Y. 1964), p. 578.
10. Lampert, M. A., *Reports on Progress in Physics* **27**, 329 (1964).
11. Helfrich, W. in *Physics and Chemistry of the Organic Solid State*, Vol. III, D. Fox, M. M. Labes and A. Weissberger, Editors (Interscience Publishers, 1967), p. 1.
12. Avakian, P., Abramson, E., Kepler, R. G., and Caris, J. C., *J. Chem. Phys.* **39**, 1127 (1963).
13. Sharp, J. H., and Schneider, W. G., *J. Chem. Phys.* **41**, 3657 (1964).
14. Bree, A., and Lyons, L. E., *J. Chem. Soc.* 2662 (1956).
15. Craig, D. P., and Hobbins, P. C., *J. Chem. Soc.* 2309 (1955).

16. Castro, G., and Hornig, J. F., *J. Chem. Phys.* **42**, 1459 (1965).
17. Chaiken, R. F., and Kearns, D. R., *J. Chem. Phys.* **45**, 3966 (1966).
18. Pope, M., and Burgos, T., *Molecular Crystals* **1**, 395 (1966).
19. LeBlanc, O. H., *J. Chem. Phys.* **35**, 1275 (1961).
20. Silby, S., Jortner, J., Rice, S. A., and Vala, M. T., *J. Chem. Phys.* **42**, 733 (1965).